MICROSTRUCTURE OF COMPOSITIONALLY MODULATED InAlAs

R.D. TWESTEN*, J. MIRECKI MILLUNCHICK*, S. P. AHRENKIEL†, YONG ZHANG†, S.R. LEE*, D.M. FOLLSTAEDT*, A. MASCARENHAS†, AND E.D. JONES*

* Sandia National Laboratories, Albuquerque, NM. 87185-1056
† National Renewable Energy Laboratory, Golden, CO. 80401

ABSTRACT

We have observed spontaneous, lateral composition modulation in tensile InAlAs alloy films grown as short-period superlattices on InP (001). We have analyzed these films using transmission electron microscopy, x-ray reciprocal space mapping, and polarized photoluminescence spectroscopy. We find the growth front is nonplanar, exhibiting ~2nm deep cusps aligned with the In-rich regions of the compositionally modulated films. In addition to the measured 15nm wavelength modulation in the [110] direction, a modulation of 30nm wavelength is seen in the orthogonal [1$\bar{1}$0] direction. The photoluminescence from the modulated layer is strongly polarized and red shifted by 0.22eV.

INTRODUCTION

Systems of reduced dimensionality have many interesting optical and electronic properties. Two-dimensional systems (i.e. quantum wells) are readily produced during growth by modulating the deposited materials. One-dimensional systems, however, prove more difficult. Many methods have been attempted, including etch and regrowth, growing on patterned and vicinal surfaces, and direct writing of lines[1]. The method we focus on is the use of spontaneous, lateral modulation in conjunction with growth modulation to form one-dimensional quantum wires. This method was pioneered by Cheng et al.[2] using strain-balanced short-period superlattices (SPS), in which each layer of the superlattice is highly strained yet of opposite sign, so the entire system is nominally lattice matched.

It has been suggested that surface relaxation can cause normally miscible systems to phase separate[3] due to the reduction of the coherency energy associated with the change in lattice constant of the separated materials. Surface relaxation also affects lattice-mismatched films where a rippling or islanding of the growth surface can lower the strain energy of the film[4] due

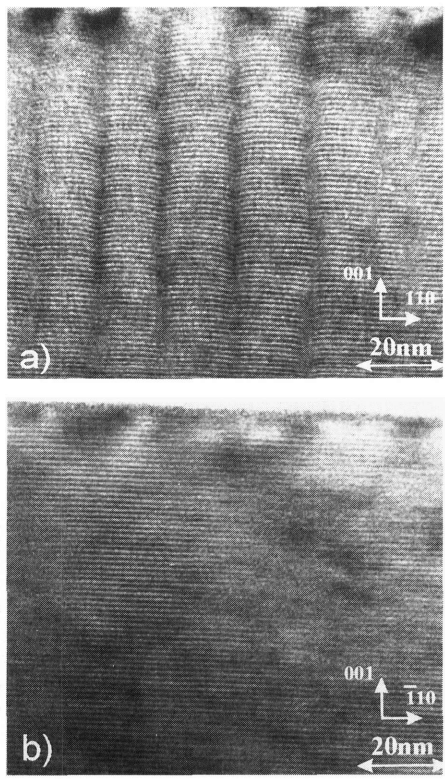

Figure 1: Bright-field TEM image in a) the [1$\bar{1}$0] projection and b) the [110] projection. The dark-vertical bands in a) are In-rich regions. The SPS is seen as horizontal lines in both images, but in a) it is cusped, indicating a nonplanar growth front.

Mat. Res. Soc. Symp. Proc. Vol. 441 © 1997 Materials Research Society

to the removal of lateral constraints afforded by the nonplanar surface.

We have observed that in Al-rich InAlAs films grown on InP(001) substrates an anisotropic, nonplanar surface has develops during growth, and the elastic relaxation of the surface correlates with the observed composition modulation (CM) in the resulting film.

EXPERIMENTAL

Material is grown directly on InP(001) wafers using molecular beam epitaxy. The InP surface is prepared by heating the surface under an As over pressure. Various structures were grown but typically consist of an approximately lattice matched InAlAs, randomly deposited buffer layer, followed by different strained regions of InAlAs either randomly deposited or grown as an SPS by alternate shuttering of the group-III element sources. Some samples also contain a randomly deposited cap. The growth rate is calibrated *in situ* using reflection high-energy electron diffraction, and the final composition is determined *ex situ* using x-ray diffraction. Here, we will focus on one film (sample 511H) grown at a substrate temperature of 540°C and a growth rate R=0.68 ML/s for the buffer layer and R/2 for the SPS. The SPS had an average structure of $(InAs)_{1.65}/(AlAs)_{1.91}$ giving an average composition of $Al_{0.54}In_{0.46}As$ while the buffer layer has a composition of $Al_{0.49}In_{0.51}As$.

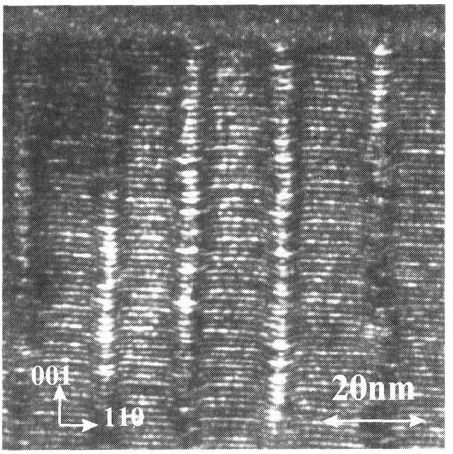

Figure 2: Dark-field (002) image of the SPS structure. The narrow bright bands centered on the SPS cusp are In-rich regions. The black -white-black variation across the In-rich regions is due to a zero in the (002) structure factor for a composition of 52% indium.

The films are characterized using transmission electron microscopy (TEM), polarized photoluminescence (PPL), and x-ray reciprocal space mapping. TEM samples were prepared either in cross-section, using mechanical polishing followed by Ar-ion milling, or in plan-view, by back-thinning with a selective chemical etch to remove the substrate, followed by Ar-ion milling. Images were obtained using either 200keV or 300 keV electrons.

RESULTS

TEM Results

Figure 1a) shows a bright-field TEM image of a region of the SPS film in the $[1\bar{1}0]$ projection, while Figure 1b) shows the same film in the 110 projection. The two projections have very different images: Figure 1a) clearly shows dark vertical bands with a spacing of approximately 13nm in the [110] direction, while Figure 1b) shows a more uniform image. The other strong feature in Figure 1 is the 3.56ML-period SPS, where one monolayer (1ML) is taken as the distance between the (002) crystal lattice planes (~2.93Å). In Figure 1b), the SPS appears as flat lines parallel to the surface, but in Figure 1a), the SPS shows strong cusps at the dark bands. Since the SPS layers are deposited in a serial fashion, they act as marker layers delineating the growth front as a function of time. Figure 1a) clearly indicates the nonplanar nature of the growth surface. For a tensile film with a nonplanar surface, we would expect the least constrained part of the surface (the film apices) to relax to a smaller lattice parameter and the troughs to be under

a larger tensile strain. This would lead to enhanced incorporation of the smaller lattice parameter alloy (Al-rich) on the tops of the islands, while the larger lattice parameter alloy (In-rich) would form in the troughs[5].

The troughs were identified as In-rich by imaging in the dark-field (002) 2-beam mode. In this mode, the contrast can be simply interpreted in terms of changes in the local structure factor[6]. The resulting image (Figure 2) shows strong black-white-black contrast in the regions of the SPS cusps. Since the average film composition is $Al_{0.54}In_{0.46}As$, increasing In composition implies decreasing image intensity until the local composition reaches $Al_{0.48}In_{0.52}As$.[7] At this point, the average group-III scattering factor exactly cancels the group-V scattering factor, causing the (002) structure factor to be kinematically forbidden. A further increase in In composition causes increasing image intensity, resulting in the bright bands surrounded narrow dark bands seen in the image. TEM image simulation for a simple composition profile is shown in Figure 3. Since the average composition of the film and the critical composition are known, we can make a first order approximation of the magnitude of the composition modulation. Assuming a simple triangular profile, the Al-rich area has a composition of $In_{0.31}Al_{0.69}As$ while the In-rich region has a composition of $In_{0.73}Al_{0.27}As$. This is probably an artificially large deviation; however, we can say the In-rich regions contain at least 52% In based on the zero in the (002) structure factor. We have simulated bright-field images also, but the difficulty of including the high-angle scattering has allowed only limited success.

The lack of strain contrast in these images is evidenced by switching from an (002) to an (004) two-beam type image. If strain were causing the image contrast, the (004) images would look similar to the (002) images. On the other hand, the (004) reflection is rather insensitive to the local group-III composition, so the resulting images will show different contrast effects. Comparison of the two images in Figure 4 indicates that structure factor contrast dominates the (002) images.

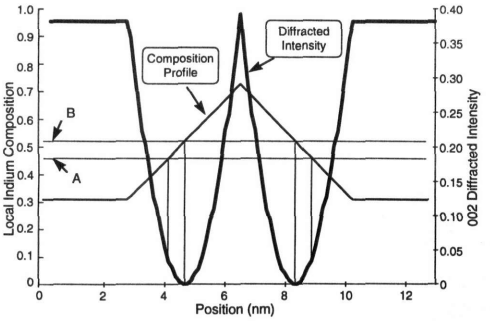

Figure 3: Semi-quantitative contrast analysis of (002) image. The diffracted intensity is computed using the column approximation for the (002) systematic row of reflections. The input composition profile is consistent with the position of the structure factor zeros and the average film composition, but is otherwise arbitrary. The line marked A is the average film composition and the line marked B is 52% indium.

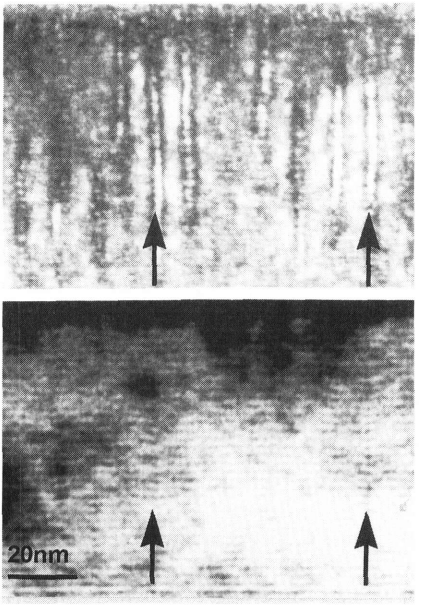

Figure 4: (002) {top} and (004) {bottom} dark-field images of the same region of the sample. Note the lack of contrast in the (004) image, indicating the contrast is dominated by structure factor variations. Equivalent positions are marked by black arrows.

The interpretation of the narrow regions as In-rich is also supported by lattice imaging. A laterally modulated structure is equivalent to a strained-layer superlattice in the [110] direction. In order to preserve lattice coherence, each layer must be lattice matched in the [001] and $[1\bar{1}0]$ directions but show tetragonal distortion in the [110] direction, with the In-rich regions being expanded and the Al-rich regions compressed. Figure 5 shows a $[1\bar{1}0]$ zone-axis lattice image of this material. The In-rich regions show dilation, seen as a bending of the {111} lattice planes, as expected for an In-rich region. Quantitative interpretation of the dilation is difficult due to the relaxation of the strain at the free surfaces of the thin foil sample[8] and short extent of the CM in the projected $[1\bar{1}0]$ direction (see below). However, the expected tetragonal distortion is observed consistently throughout the sample.

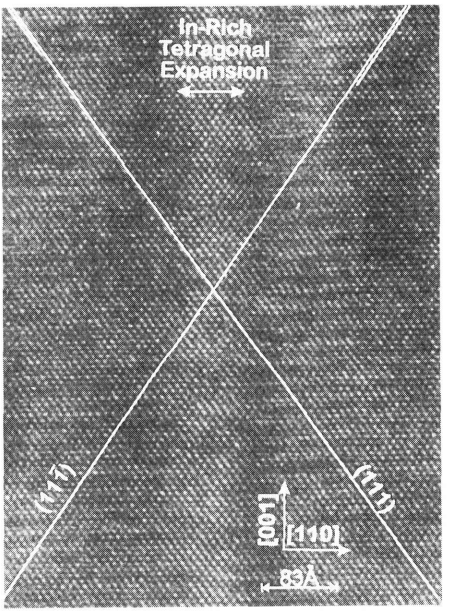

Figure 5: $[1\bar{1}0]$ zone-axis lattice image of an In-rich region showing tetragonal distortion of the lattice, which appears as an offset of the (111) planes as the In-rich region is crossed. The (002) lattice planes are flat, as expected, and the SPS cusping can be weakly seen. The lines in the figure are drawn to follow the {111} planes from the Al-rich regions in the lower portion of the figure, through the In-rich center portion of the figure. The approximate offset of the corresponding {111} planes in the opposite Al-rich region of the film is indicated by the second line in the upper portion of the figure.

Polarized Photoluminescence

In samples showing composition modulation (CM), the symmetry of the cubic lattice has a superposed envelope function modulation. Because the binary constituent alloys are lattice mismatched, this envelope function modulation has two components: one related to the lateral composition oscillation, and the other to the associated strain oscillation. As mentioned above, the axis for the tetragonal distortion associated with the strain oscillation is parallel to that of the composition oscillation[9]. The axis of the lateral CM thus becomes a preferred symmetry axis, and it is expected that this symmetry lowering will be reflected in the electronic band structure. The interband electronic transitions in the SPS structure are expected to show preferred polarization along the CM axis. In accordance with previous studies[9] on compositionally modulated material, it is expected that band-edge electron-hole recombination will occur at lower energies as compared to the disordered $InAlAs_2$ alloy. To study these effects, low temperature polarized photoluminescence (PPL) measurements were performed.

Figure 6 shows the low-temperature PPL spectra taken at 10K, using the 514.5nm line of an Ar ion laser with a power of 3mW. The PPL emission was analyzed with a polarizer parallel to either [110] or $[\bar{1}10]$, and another polarizer parallel to [100] was placed just in front of the spectrometer to eliminate the effect of the polarization-dependent throughput of the spectrometer. The luminescence signal was dispersed by a 0.27m single-grating spectrometer and detected with a CCD detector array. The strong peak at 1.32eV comes from the SPS layer, while the peak at 1.54eV originates from the alloy buffer layer. This was established by selectively removing first the SPS and then the buffer and examining the PPL spectra for each case. The PPL emission

from the SPS is red shifted by 0.22eV with respect to the emission from the buffer[10] and is strongly polarized, with a polarization ratio of ~20. The photoluminescence from the buffer is also polarized with an anisotropy of ~10. This may be due to the fact that the buffer layer shows double variant CuPt ordering, which gives rise to Orientational Superlattice effects[11]. TED patterns from the buffer show two pairs of ½(111) diffraction spots associated with CuPt ordering along the two $[111]_B$. These spots appear elongated along the [001] direction, indicating the existence of a superposed modulation along this axis which is essentially the Orientational Superlattice. In single variant CuPt alloys, the anisotropy of the PPL is always less than 3, but in Orientational Superlattices this value has been predicted[12] to be much larger than 3, as observed here.

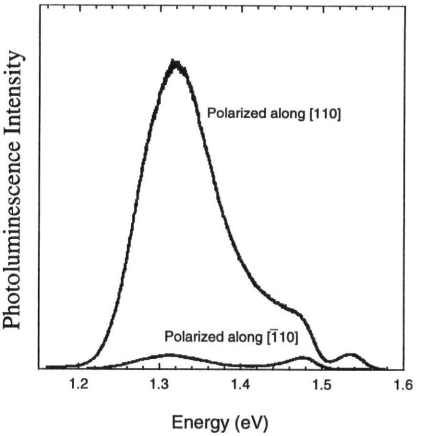

Figure 6: Low-temperature PL spectra taken at 10K. The polarization of the PL emission is indicated on the figure.

X-ray Diffraction Results

Figure 7 shows the diffracted intensity in reciprocal space around the {224} reflections recorded using Cu-Kα x-rays and a position-sensitive detector[13]. In the left panel, the scattering vector has a component parallel to the [110] direction, while in the right panel, it is parallel to the [1$\bar{1}$0] direction. In both cases, the tensile nature of the film is revealed by the tetragonal distortion of the lattice parallel to [001]. The increase in length of the film's (004) reciprocal lattice vector by 0.801% over that of the InP substrate indicates a tensile film with an average composition of $Al_{0.54}In_{0.46}As$.

Both incident directions show lateral satellites off the {224} SPS reflections, indicating the films are modulated in the <110> directions. However, the [110] modulation has an average period of 15nm, while in [1$\bar{1}$0] the modulation is 35nm. Based on XTEM results, the modulation in the [1$\bar{1}$0] was unexpected. However, plan-view TEM images (not shown) of the same film show evidence for modulation in the [1$\bar{1}$0] direction. The lack of contrast in the cross-sectional images may be due to a specimen thickness that superimposes several modulations.

We should note the lateral modulation of the x-ray signal was not observed around the (004) reflection and was seen only weakly around (002) (whose structure factor has a stronger chemical dependence). However, upon switching to a reflection that has a {110}

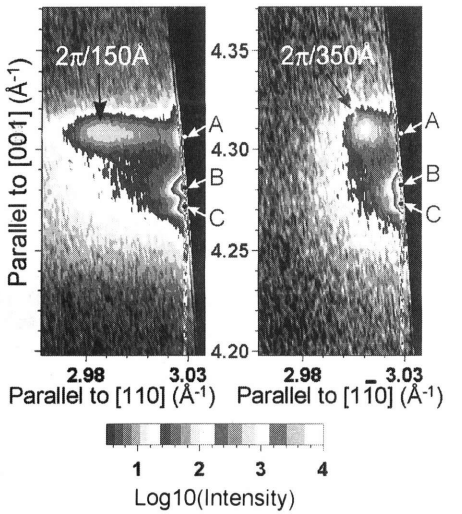

Figure 7: X-ray reciprocal space maps around inside half of the {224} reflections. Lateral modulation is seen in both projections. However, the modulation has a shorter period in the [110] direction. The symbols marked A,B & C are the SPS, buffer & substrate {224} reflections, respectively.

component, such as {224}, the purely chemical modulation of the symmetric reflections is enhanced by coupling into the tetragonal lattice modulation of the {hh0} planes which accompanies the chemical modulation.

CONCLUSIONS

The importance of strain energy to film composition has been a long-standing problem[14]. The reduction of strain energy due to surface relaxation has been applied to both spinodal decomposition[3] and to the equilibrium morphology of strained films[4]. In studying Al-rich InAlAs films, we have observed not only lateral CM but also the correlation of growth front islanding and relaxation to resulting bulk film CM.

The cross-section TEM images and diffraction have shown that the films are compositionally modulated, and imaging the SPS indicates the surface has become nonplanar. Careful analysis of the image contrast reveals that the apices of the surface islands are Al-rich while the troughs between the islands are In-rich. This is in agreement with the expected surface relaxation and the resulting gradient in the surface chemical potential for a tensile film. X-ray diffraction and plan-view TEM, however, reveal that the film is compositionally modulated in both the <110> directions. The wave-length of the modulation is shorter in the [110] direction (150Å) than in the $[1\bar{1}0]$ direction (350Å). This anisotropy is probably due the to the 2-fold symmetry of the As-terminated surface, which has a higher surface mobility in the $[1\bar{1}0]$ direction than in the [110]. Since the modulation is strongly coupled to the surface mobility, the observed structure is probably kinetically limited rather than in equilibrium.

The PPL results show a red shift of the band edge transitions in the compositionally modulated film. The signal is strongly polarized in the [110] direction with an anisotropy ratio of ~20. The PPL emission from the unmodulated buffer occurring at 1.54eV also shows an anisotropy (~10). This anisotropy, however, is attributed to CuPt ordering in the buffer layer, which has been verified using electron diffraction.

This work was supported by the U.S. Department of Energy under contract DE-AC04-94AL85000 and by its Office of Basic Energy Sciences. Sandia is a multiprogram laboratory operated by Sandia Corporation, a Lockheed Martin Company, for the U.S. Department of Energy.

REFERENCES

1. See for example: E. Kapon, Proc. IEEE **80**, 398 (1992).
2. K. Y. Cheng, K. C. Hsieh and J. N. Baillargeon, Appl. Phys. Lett. **60**, 2892 (1992).
3. F. Glas, J. Appl. Phys. **62**, 3201 (1987).
4. D. J. Srolovitz, Acta Metall. **37**, 621 (1989).
5. J. E. Guyer and P. W. Voorhees, Phys. Rev. B **54**, 11710 (1996).
6. M. M. J. Treacy, J. M. Gibson, and A. Howie, Phil. Mag. **A51**, 389 (1985).
7. Due to the weak nature of the (002) reflection, contrast reversals due to dynamic diffraction are not expected.
8. J. M. Gibson and M. M. J. Treacy, Ultramicroscopy **14**, 345 (1984).
9. A. Mascarenhas, R. G. Alonso, G. S. Horner, S. Froyen, K. C. Hsieh, and K. Y Cheng, Superlattices and Microstructure **12**, 57 (1992).
10. Since the film is Al-rich, we would expect a blue shift based on composition arguments only.
11. A. Mascarenhas, Yong Zhang, R.G. Alonso and S. Froyen, Solid State Comm. **100**, 47 (1996).
12. Yong Zhang and A Mascarenhas, (to be published).
13. S.R. Lee, B.L. Doyle, T.J. Drummond, J.W. Medernach and R.P. Schneider, Jr., in Advances in X-Ray Analysis Vol.38 edited by P. Predecki et al. Plenum Press, New York, 1995), p. 201-213.
14. J. W. Cahn, Acta Met. **9**, 975 (1961).